

# Influence of FRP Strengthening on Structural Performance of Shear Deficient RC Beams with Varying Degree of Corrosion

Arjun Hari<sup>1</sup>, Jayalekshmi S<sup>2</sup>, Safrin Saif<sup>3</sup>, Preetha Prabhakaran<sup>4</sup>

<sup>1,2,3</sup>Student, Department of Civil Engineering, Toc H College of Engineering Arakkunnam

<sup>4</sup>Assistant Professor, Department of Civil Engineering, Toc H College of Engineering Arakkunnam,

## Abstract

Corrosion of beams, particularly in structural applications such as bridges, buildings, or other infrastructure, can lead to significant safety hazards and structural integrity concerns. The corrosion of beams can occur due to various environmental factors and conditions, and the type of corrosion can vary depending on the specific circumstances. This paper investigates the structural behaviour of shear-deficient reinforced concrete (RC) beams by characterizing material properties, assessing compressive strength, and casting beams designed to exhibit shear deficiencies. The study explores the effects of inducing varying degrees of corrosion through accelerated corrosion techniques, followed by the application of Carbon Fiber Reinforced Polymer (CFRP) sheets for strengthening. The structural performance of corroded shear deficient RC beams are evaluated before and after FRP strengthening.

**Keywords:** Shear deficient, CFRP sheets, Pre cracking, Energy ductility

## 1. Introduction

Reinforced concrete (RC) structures are susceptible to various forms of deterioration over their service life, including corrosion-induced deterioration and deficiencies in shear capacity, which can compromise structural integrity and safety. Shear deficiencies in RC beams often result from inadequate design or construction practices, leading to potential failure under lateral loads. Additionally, corrosion of steel reinforcement due to environmental exposure can significantly reduce the load-carrying capacity and durability of concrete elements, particularly in coastal or industrial environments with high chloride concentrations. To address these challenges, the use of Carbon Fiber Reinforced Polymer (CFRP) sheets for strengthening has emerged as a viable retrofitting technique to enhance the performance of deteriorated RC structures. This experimental study aims to investigate the effectiveness of CFRP strengthening in restoring and enhancing the shear capacity of shear-deficient RC beams subjected to varying degrees of corrosion. By characterizing material properties, inducing controlled pre-cracking, simulating accelerated corrosion, and applying CFRP sheets, this study seeks to provide valuable insights into rehabilitation strategies for shear-critical RC structures exposed to corrosive environments.

## 2. Experimental Investigation

The test program included eight beams categorized into four groups depending on the degrees of corrosion (0%, 5%, 10%, 15%): UB0, UB5, UB10, UB15 and SB0, SB5, SB10, SB15. The SB group included

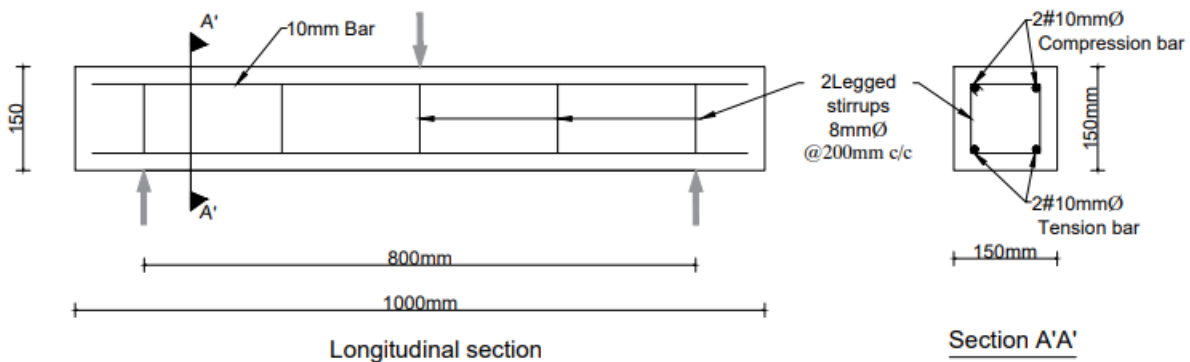
strengthened and UB group included un strengthened beams. After 28 days of curing , the eight beams were subjected to three-point bending test to induce pre-cracks and then six beams were exposed to varying degrees of accelerated corrosion(0% ,5%,10%,15%). The pre-cracking and accelerated corrosion were designed to induce a combination of pitting and general corrosion in tensile reinforcement, considered a proper representation of the practical corrosion problems. After the corrosion period, one beam in each group was kept as un-strengthened, and the other beams group were strengthened with CFRP laminates bonded to the tensile bottom of the beam. Further details of the experimental program are described in the following sections.

**2.1. Design and casting of RC beams**

The RC beam (1000 x 150 x 150 mm) is designed as per IS 456: 2000. Figure 1 shows the dimensions of the beams and the position of steel reinforcement. Each beam was reinforced with two ribbed 10 mm bars in the tension zone and two ribbed 10mm bars in the compression zone. Stirrups of 8mm diameter were placed at a spacing of 200 mm with clear concrete cover of 25 mm. The wires from tensile reinforcement is connected to impressed current source for accelerated corrosion. It assured a well-defined exposure area of steel rebars to artificial electrochemical corrosion, based on which the magnitude of the impressed current was determined, to obtain expected corrosion level of tensile rebars over a certain period. After casting, the beams were placed in the curing tank in an indoor climate for 28 days.

All specimens were eventually subjected to structural testing until failure to investigate their load deflection behavior and failure modes.

**Figure 1: Dimensions and cross-section of the reinforced concrete beams casted**



**2.2 Pre-cracking of RC beams**

After 28 days of curing, the eight beams were subjected to three-point bending test with an effective span of 800 mm and pre-loaded to 48.87 kN. The maximum pre-load was equivalent to 60% of the theoretical yielding load, representing a reasonable load level in serviceability limit state. The pre-loading induced pre-cracks to provoke pitting corrosion in the subsequent accelerated corrosion period.

Pre cracking load = 60% of ultimate load

$$= \frac{60 \times 81.45}{100} = 48.87kN$$

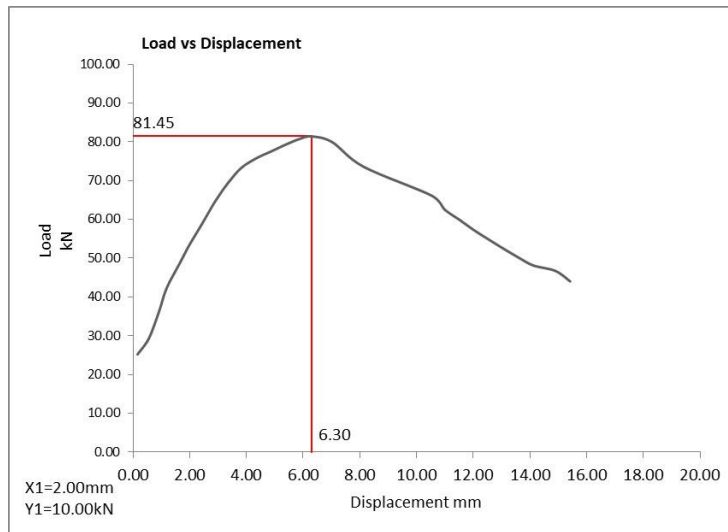
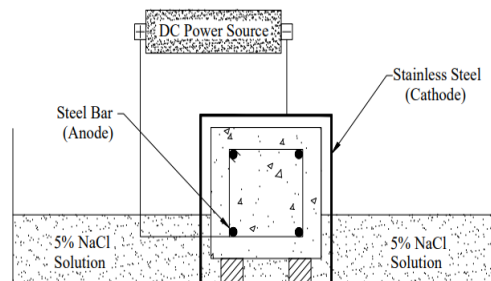


**Figure 2: Load displacement graph of Ultimate load test**

### 3. Accelerated corrosion technique

The primary goal of accelerated corrosion techniques is to subject materials to harsh environmental conditions in a controlled laboratory setting, causing them to corrode at a much faster rate than they would under normal circumstances

**Figure 3: Schematic diagram of accelerated corrosion technique**



After application of pre-cracking load, all the beams to be strengthened are corroded using accelerated corrosion technique. To accelerate the corrosion process for the tension steel reinforcement, salt (NaCl) solution was added to the mixer before concrete casting so that 3% chloride ions, by weight of cement, were uniformly distributed along the bottom third of each specimen to be corroded. Set-ups used for inducing reinforcement corrosion through accelerated corrosion process consist of a DC power source, a counter electrode, and an electrolyte. The stainless steel plate located at the side of each specimen acted as the cathode for this corrosion process, whereas the tension reinforcing bars acted as the anode. The positive terminal of the DC power source is connected to the steel bars (anode) and the negative terminal is connected to the counter electrode (cathode) which is the stainless-steel plate. Accelerated corrosion was carried out by impressing an electric current through the main longitudinal bottom reinforcing bars of about 500 mA, which corresponds to approximate current density of 884.64 A/cm<sup>2</sup>. The current is impressed from counter electrode to the rebars through concrete with the help of the electrolyte (normally 5% NaCl solution). The level of salted water was 110 mm, which submerged 10 mm of the bottom of beam specimen. Figure 3 explains the schematic diagram of accelerated corrosion setup.

To estimate the approximate mass loss associated with this corrosion process, Faraday’s law was used. Impressed current calculations are presented in Table 1. To obtain theoretical mass loss of 5% in tension reinforcement rebar of specimen, a constant current of 500 mA was applied to each specimen for a period of 5 days. Therefore, a constant current of 500 mA was applied to each specimen for a period of 7 days, to obtain theoretical mass loss of 10% in tension reinforcement rebar of specimen. Likewise, to obtain theoretical mass loss of 15% in tension reinforcement rebar of specimen, a constant current of 500 mA was applied in each specimen for a period of 13 days.

This current density was obtained by dividing the total impressed current by the surface area of the portion of the steel reinforcement cage that is in the salted concrete (specimen’s bottom third). During construction of the specimens, the tension reinforcing bars were tied up with electrical wires extended about 60 mm out of each specimen from one end to facilitate connection to the power supply.

The specimens and stainless-steel plate were connected in parallel to the power supply. As shown in Figure.4, specimen were placed in a brick made tank with size of 3000 mm long, 2500 mm wide and 500 mm height which contained salted water (5% of salt). The corrosion current was monitored daily, and any drift was corrected.

**Table 1: No. of days required for corrosion**

Degree of corrosion	5%	10%	15%
Length of exposed tensile steel in concrete (mm)	900	900	900
Diameter of rebar (mm)	10	10	10
Cross-sectional area of rebar (mm <sup>2</sup> )	78.6	78.6	78.6
No. of rebars	2	2	2
Volume of tensile steel (mm <sup>3</sup> )	141480	141480	141480
Surface area (mm <sup>2</sup> )	56520	56520	56520
Mass of steel in salted concrete (g)	1110.62	1110.62	1110.62
Percentage of mass loss (%)	5	10	15
Mass loss (g)	55.53	111.06	166.6
<b>Current</b> (Knowing that 1 A h consume 1.04 g of Iron using Faraday’s law)			
Ampere hour (Ah) required for the mass loss	53.4	106.78	160.2
No. of hours required with current of 500mA (h)	106.8	213.56	320.4
No. of days	5	7	13
Applied current (mA)	500	500	500
Current density (IA/cm <sup>2</sup> )	884.64	884.64	884.64

Figure.4: Experimental setup



#### 4. Strengthening of RC beams using CFRP

Before bonding the composite fabric onto the concrete bottom surface, the required region of concrete surface was made rough using a coarse sand paper texture and cleaned with an air blower to remove all dirt and debris. Once the surface was prepared to the required standard, the epoxy resin was mixed in accordance with manufacturer's instructions (1:1 ratio). Mixing was carried out in a plastic container and was continued until the mixture was in uniform colour. When this was completed and the fabrics had been cut to size (900 mm x 100mm x 0.41 mm), the epoxy resin was applied to the tensile bottom of the concrete surface. The composite fabric was then placed on top of epoxy resin coating and the resin was squeezed through the roving of the fabric with the roller. Air bubbles entrapped at the or epoxy/fabric interface were to be eliminated. During hardening of the epoxy, a constant uniform pressure was applied on the composite fabric surface in order to extrude the excess epoxy resin and to ensure good contact between the epoxy, the concrete and the fabric. This operation was carried out at room temperature. Concrete beams strengthened with CFRP were cured for 24 hours at room temperature before testing.

Figure 6 Dimensions and cross-section of the CFRP bonded reinforced concrete beam

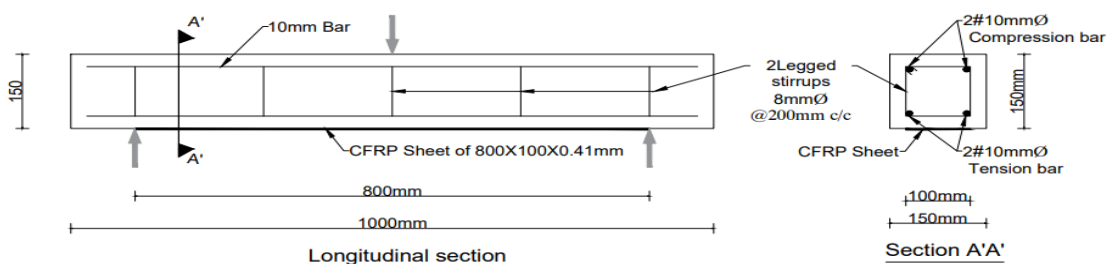


Figure 7 Epoxy resin



Figure 8 Strengthened RC beams using CFRP sheets



### 5. Load Deflection Behaviour

Test results present the experimental findings related to strengthening of corroded RC beams using CFRP laminate. Load-displacement behavior was characterized through the presentation of load-displacement graph, highlighting its ultimate load and corresponding deflection. The observed failure modes including concrete crushing, shear failure, and CFRP debonding in strengthened corroded beams were analyzed to understand how CFRP reinforcement influenced the failure mechanisms compared to uncorroded beams. *Ductility* was assessed through post-peak behavior analysis, considering displacement ductility ratios. The results obtained from the experimental tests are shown in Table 2.

Table 2 Summary of test results

Sl No	Beam ID	Ultimate load (kN)	% decrease in ultimate load with increase in degree of corrosion	% increase in ultimate load w.r.t. unstrengthened beam
1	UB0	81.4	-	12.16
2	SB0	91.3	-	
3	UB5	76.1	6.51	13.14
4	SB5	86.1	5.70	
5	UB10	70.9	12.89	



6	SB10	82.6	9.52	16.5
7	UB15	66.2	18.67	22.9
8	SB15	81.4	10.8	

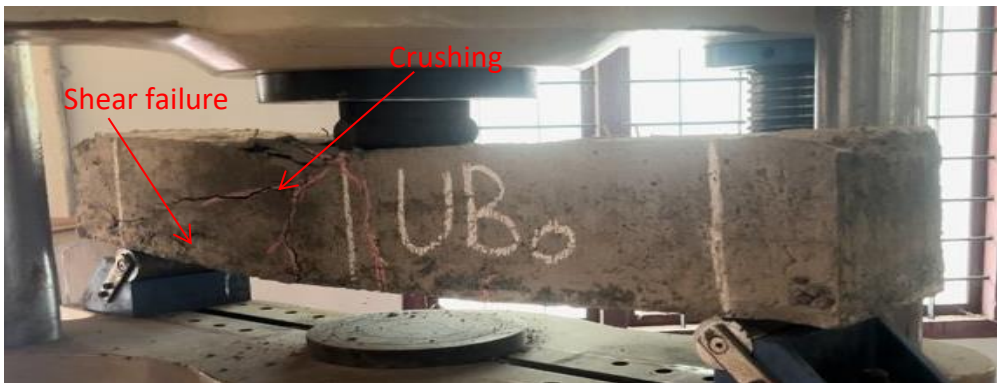
Pu = ultimate load , UB =un-strengthened beams , SB=strengthened beams

### 5.1. Failure modes

All the specimens were failed in shear. The diagonal shear cracks were clearly visible on the sides of the beam. Similar crack pattern was also visible for strengthened specimens confirming that all the beams were failed in shear. In UB0, the failure occurred with the combination of diagonal shear failure and concrete crushing near the point of action of load. Whereas in SB10 and SB15 flexural failure also occurred.

**Figure 9 Failure modes of strengthened and un-strengthened RC beams**

(a)UB0



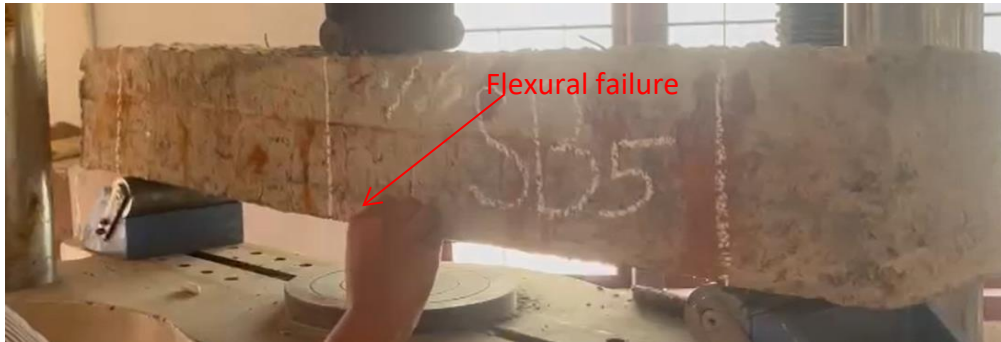
(b)SB0



(c)UB5



(d)SB5



(e)UB10



(f)SB10



(g)UB15





(h)SB15



**Table 3 Observed failure modes**

Sl.No	Specimen ID	Mode of failure
1	UB0	Shear failure & crushing
2	SB0	Shear failure
3	UB5	Shear failure
4	SB5	Flexural failure
5	UB10	Shear failure
6	SB10	Flexural failure
7	UB15	Shear failure
8	SB15	Flexural failure

### 5.6. Effect of Strengthening on Ductility

Ductility of a member is defined as its ability to sustain large inelastic deformations prior to failure without substantial loss of strength. It is a desirable structural property because it allows stress distribution and provides warning of impending failure. These quantities are expressed as indices or factors, through relationship at two different stages, namely, at yielding of the tension steel and at ultimate load capacity. Energy ductility of beams is calculated as ratio of energy absorbed till failure divided by the energy absorbed till first steel yielding. Ductility ratio is calculated as the percentage of ductility of the strengthened beam divided by that of the un-strengthened beam. Thus, ductility indices can be expressed as:

$\Delta_u$ - Deflection at Ultimate Load (mm)

$\Delta_y$  - Deflection at Yield Load (mm)

$\mu_\Delta$ - Deflection Ductility

$$\mu_\Delta = \frac{\Delta_u}{\Delta_y}$$

$E_u$ - Energy absorbed upto Ultimate Load (kN-mm)

$E_y$ - Energy absorbed upto Yield Load (kN-mm)

$\mu_E$ - Energy Ductility

$$\mu_E = \frac{E_u}{E_y} \text{ Ductility ratio}$$

$$\text{Ductility ratio} = \frac{\text{Ductility of strengthened specimen}}{\text{Ductility of control specimen}} \times 100$$

**Table 4 Energy ductility index of beam**

Specimen	Ultimate load kN	$E_u$ mm	Yield load kN	$E_y$ mm	$\mu_E$	Ductility ratio
UB0	81.4	440.72	79	347.68	1.27	3.28
SB0	91.3	781.716	75	187.09	4.17	
UB5	76.1	399.971	70.6	242.82	1.64	1.62
SB5	86.1	468.13	74	175.72	2.66	
UB10	70.9	349.91	55	106.91	3.27	1.1
SB10	82.6	508.84	53.8	141.10	3.6	
UB15	66.2	499.28	53.2	119.78	4.16	1.18
SB15	81.4	454.72	54	92.12	4.93	

From Table 4, it can be observed that energy ductility ( $\mu_E$ ) of strengthened beams is higher than that of un strengthened beams, which indicates that the strengthened beam is not undergoing brittle failure (due to involvement of the strengthening material ,CFRP laminate which is a brittle material ).The higher energy ductility index indicates the delay and prevention of brittle failure by allowing the beam to deform plastically before reaching the ultimate failure. The results also indicated that for higher degree of corrosion (10% and 15%), energy ductility ratio maintains the same value ( approximately 1.2%) . This is due to the fact that because of the higher tensile strength , the involvement of CFRP laminate in carrying the load after steel yielding is higher in corroded beams with higher degree of corrosion.

## 6. Conclusion

The following major conclusions are drawn based on the experimental studies carried out under this investigation.

- The use of CFRP sheets for strengthening RC beams is capable of maintaining structural integrity and increasing the ultimate strength of these beams to a level above the ultimate strength of the control beam.
- The study has shown the effectiveness of CFRP strengthening in restoring and enhancing the structural performance of corroded reinforced concrete beams across a range of corrosion levels.
- The higher energy ductility index of strengthened beams indicates the delay and prevention of brittle failure by allowing the beam to deform plastically before reaching the ultimate failure.
- The increasing improvement with higher degrees of corrosion highlights the critical role of advanced rehabilitation techniques in extending the service life and reliability of deteriorated infrastructure.

## References

1. Al-Saidy A.H , A.S. Al-Harthy , K.S. Al-Jabri , M. Abdul-Halim , N.M. Al-Shidi (2017) “Structural performance of corroded RC beams repaired with CFRP sheets”, Composite Structures , Volume 92, Issue 8 , 1931-1938

2. **Garyfalia G. Triantafyllou Theodoros C. Athanasios I. Karabinis** (2018) “Effect of patch repair and strengthening with EBR and NSM CFRP laminates for RC beams with low, medium and heavy corrosion” , Composites Part B: Engineering .Vol.133, 101-111
3. **Manikandan R.K , Shunmugapriya K, et al** (2022) “Retrofitting of reinforced concrete beams using CFRP with various adhesive” , Materials Today: Proceedings Vol:68 ,1635-1640
4. **Sadiqul Islam GM, F. H. ChowdhuryA. DevIsmawi** ( 2021) , “Pre-cracked RC Beam Strengthening With CFRP Materials” , IEEE Vol:10 ,1-4
5. **Sandeep S. Mahendrakar, Tejas D. Doshi, V.D. Gundakalle** (2023) , “Behaviour of carbon fibre reinforced polymer strengthened and retrofitted RC beams” , Materials Today: Proceedings Vol.88, Part 1, 160-168.
6. **Thang Do-Dai Tu Chu-Van, Duong T. Tran, Ayman Y. Nassif** (2022) “Efficacy of CFRP/BFRP laminates in flexurally strengthening of concrete beams with corroded reinforcement” , Journal of Building Engineering. Vol.53
7. **Yiyuan Wang and Jin Wu** (2023), “Flexural Behavior of Corroded Concrete Beams Strengthened with Carbon Fiber-Reinforced Polymer ” , MDPI Vol:16(12) ,1635-1640